Journal of Photochemistry and Photobiology A: Chemistry 219 (2011) 148–153

Contents lists available at ScienceDirect

Journal of Photochemistry and Photobiology A: Chemistry

journal homepage: www.elsevier.com/locate/jphotochem

Benzimidazole derivatives in the electrolyte of new-generation organic dye-sensitized solar cells with an iodine-free redox mediator☆

Jungsik Min[a], Jongok Won[a,*], Yong Soo Kang[b], Shigeru Nagase[c]

[a] Department of Chemistry, Sejong University, 98 Gunja, Gwangjin, Seoul 143-747, Republic of Korea
[b] WCU Department of Energy Engineering, Hanyang University, 1 Haengdang, Seongdong, Seoul 133-791, Republic of Korea
[c] Department of Theoretical Molecular Science, Institute for Molecular Science, Okazaki, Aichi 444-8585, Japan

ARTICLE INFO

Article history:
Received 16 December 2010
Received in revised form 26 January 2011
Accepted 1 February 2011
Available online 1 March 2011

Keywords:
Benzimidazole additives
Electrolyte
DSSC
TEMPO
Organic dye

ABSTRACT

The effect of the addition of benzimidazole derivatives (*x*BI) to new-generation organic dye-sensitized solar cells (DSSCs) was investigated by measuring the photovoltaic performance and by using a theoretical approach. An organic indoline dye (D149) and a stable organic radical, 2,2,6,6-tetramethyl-1-piperidinyloxy (TEMPO), were employed as the sensitizer and redox mediator, respectively, for the fabrication of DSSCs. Three different *x*BI additives were added to the electrolyte with and without bis(trifluoromethane) sulfonimide lithium salt (LiTFSI) in D149-DSSCs with a TEMPO/TEMPO$^+$ redox mediator. Competitive adsorption occurred significantly between D149 and *x*BI on TiO_2 particles in acetonitrile without the presence of LiTFSI in the electrolyte, implying a role of Li^+ in the electrolyte of D149-DSSCs. The addition of *x*BIs increased the open-circuit voltage (V_{oc}) by the band-edge shift upward when a negative surface charge was built up on the surface of the TiO_2 particles treated with Lewis base-*x*BIs. The addition of *x*BIs in the presence of LiTFSI/acetonitrile electrolytes would increased the photocurrent by more than 40% due to the suppression of recombination on the bare surface of the TiO_2 particles by the effective shielding of Li^+ on TiO_2. The value of V_{oc} decreased due to the decreased redox potential of the redox mediators in the presence of *x*BI, which was confirmed by the theoretical and experimental methods.

1. Introduction

Recently, dye-sensitized solar cells (DSSCs) have been studied as a promising, low-cost alternative to conventional inorganic solar devices. The energy conversion in DSSCs is based on electron injection from a photoexcited state of the sensitizer (i.e., dye) attached to TiO_2 semiconductor nanoparticles into the conduction band of the TiO_2. The redox mediator is a key component of DSSCs because the oxidized sensitizers can be reduced by a redox mediator present in the electrolyte. Then, the oxidized mediators diffuse to the counter electrode, where they are reduced, such that the photoelectrochemical cell is regenerative.

The most common redox mediator used in DSSCs, the iodide/triiodide (I^-/I_3^-) couple, is soluble and provides rapid dye generation. However, it has some disadvantages, such as the corrosion of metallic grids (e.g., silver or vapor-deposited platinum) and the partial absorption of visible light near 430 nm by the I_3^- species [1]. Another drawback of the I^-/I_3^- system is the mismatch between the redox potentials in common DSSC systems [2–4] with Ru-based dyes, which results in an excessive driving force of 0.5–0.6 eV for the dye-regeneration process. Because the energy loss incurred during dye regeneration is one of the main factors limiting the performance of DSSCs, the search for alternative redox mediators with a more positive redox potential than I^-/I_3^- is a current research topic of high priority. Several studies have been conducted to find alternative redox couples, such as $SCN^-/(SCN)_3^-$ [5], $SeCN^-/(SeCN)_3^-$ [5,6], cobalt(II/III) [7,8], copper(I/II) [9] coordination complexes, and organic mediators such as 2,2,6,6-tetramethyl-1-piperidyloxy (TEMPO) [10]. Among these examples, the use of the TEMPO/TEMPO$^+$ redox mediator system in Ru-free organic dye-based DSSCs might be a promising avenue of exploration due to its easy chemical modification.

Although iodine-free redox mediators using TEMPO were shown as possible substitutes for the I^-/I_3^- system [10], the cell performance was still lower than that of the conventional DSSCs. In an attempt to improve the solar cell performance, the addition of optimum additives could be a solution. Various additives in the electrolyte of Ru dye-based DSSCs have been examined in many studies [11–15]. In one example, acids, such as acetic acid, in an I^-/I_3^- acetonitrile solution increased the photocurrent but

☆ This work was presented at the Hybrid and Organic Photovoltaics Conference (HOPV2010, May 23–27, 2010, Assisi, Italy).

* Corresponding author. Tel.: +82 2 3408 3230; fax: +82 2 3408 4317.
E-mail address: jwon@sejong.ac.kr (J. Won).

1010-6030/$ – see front matter © 2011 Elsevier B.V. All rights reserved.
doi:10.1016/j.jphotochem.2011.02.004

decreased the photovoltage [11]. On the other hand, additives, such as NH_3, 4-t-butylpyridine [12,13] or 1-methylbenzimidazole [14,15], in acetonitrile provided drastically increased photovoltage in DSSCs with a Ru-based dye and I^-/I_3^- redox couple.

Most of the additives were found by trial-and-error approaches, and there are few studies of the additive effect on the organic dye-sensitized solar cells in non-iodine redox mediators. This research aims to clarify the effects of the benzimidazole derivative (*x*BI) addition to TEMPO/TEMPO$^+$ redox mediator electrolytes on the performance of a new generation of organic dye-sensitized solar cells. The influence on cell performance was investigated by examining the photovoltaic performance of different *x*BI additives in the TEMPO/TEMPO$^+$/acetonitrile electrolyte of DSSCs and by computational calculations.

2. Experimental

2.1. Materials

The mediator 2,2,6,6-tetramethyl-1-piperidyloxy (TEMPO) was purchased from Tokyo Chemical Industry Co., Ltd. Nitrosonium tetrafluoroborate ($NOBF_4$), benzimidazole (BI), 1-methylbenzimidazole (1MB), 5-methylbenzimidazole (5MB), bis(trifluoromethane) sulfonimide lithium salt (LiTFSI), titanium(IV) chloride ($TiCl_4$), chloroplatinic acid hydrate (H_2PtCl_6), tert-butanol and isopropyl alcohol (IPA) were purchased from Aldrich. The acetonitrile was purchased from Junsei. The TiO_2 paste (18 nm, TiO_2 Paste DSL 18NR-T) was purchased from Dyesol. The indoline dye (D149) is a commercial product from Inabata & Co., Ltd. The transparent glass coated with a conductive fluorine-doped tin oxide (FTO, TEC8, 8 Ω/□) for the electrodes was purchased from Pilkington.

2.2. Fabrication

The photo electrode was prepared by depositing a $TiCl_4$ solution (40 mM in water) onto the FTO glass by spinning and heating it at 500 °C for 30 min. Then, a TiO_2 layer using TiO_2 paste was deposited using a doctor blade and then sintered at 500 °C for 30 min. The TiO_2 films were treated again with $TiCl_4$ and sintered at 500 °C for 30 min. The TiO_2 thin films (thickness of approximately 12 μm) were immersed in a 0.3 mM solution of D149 in an acetonitrile/tert-butanol mixture (v/v, 1:1) for 18 h at 30 °C. The residual dye solution was rinsed with acetonitrile and dried with N_2 gas. The Pt counter electrodes were prepared by spin coating the H_2PtCl_6 solution (0.01 M in IPA) onto the conductive FTO glass and then by sintering at 450 °C for 30 min.

The electrolyte was prepared by 0.5 M TEMPO and 0.025 M $NOBF_4$, with and without 1.2 M LiTFSI in acetonitrile. Solutions of 0.5 M of different *x*BIs were added to observe the effect of the additives. $NOBF_4$ was added to oxidize the TEMPO to TEMPO$^+$ to make the redox mediator [10]. To assemble the cells, two electrodes were sealed together by surlyn (SX1170-25, 25 μm in thickness, Solaronix) and heated in a press at 90 °C. The active area of the DSSC was 0.16 cm^2.

2.3. Characterization

The current–voltage characteristics of the DSSCs were determined under 1-sun illumination (AM 1.5 G, 100 mW cm^{-2}) with a Newport (USA) solar simulator (300-W Xe source) and a Keithley 2400 source meter using a mask with an aperture area of 0.25 cm^2. The work function of the film was measured by a photon electron spectrometer (AC-2, Riken Keiki Co., Ltd.) [16,17]. Cyclic voltammetry (CV) was performed using a computer-controlled Thales Z1.21 USB program of IM6e (Zahner® elektrik) in combination with a conventional three-electrode, one-compartment electrochemical cell (plate material evaluating cell, ALS Co., Ltd.). Platinum disks were used as the working and counter electrodes. The reference electrode was Ag/AgCl, which was calibrated by measuring the redox potential of saturated potassium chloride dissolved in the solution, and the redox potentials were converted to those versus a standard hydrogen electrode (SHE) reference scale by adding a constant of 0.1976 V. The dye detachment was investigated by an ultraviolet/visible–near infrared diffuse reflectance spectrophotometer (JASCO V-670 double-beam UV/Visible Spectrophotometer). For the UV measurement, a D149-dye attached a TiO_2 electrode film was measured before and after the exposure in 1 mL of 0.5 M of the different *x*BI/acetonitrile solutions for 1 h in a closed container. After sonication for 10 min in acetonitrile, the detached dye was rinsed off with acetonitrile, and the electrode film was dried with N_2 gas.

Table 1
Photovoltaic performance of DSSCs with different additives.

	V_{oc} (V)	J_{sc} (mA cm^{-2})	FF	η (%)	Work function (V)
–	0.211	4.21	26.21	0.23	5.93
LiTFSI 1.2 M	0.690	8.12	39.64	2.22	–
BI 0.5 M	0.860	5.77	48.42	2.40	5.95
1MB 0.5 M	0.907	4.28	43.21	1.68	5.89
5MB 0.5 M	0.924	2.95	15.4	0.42	5.84

2.4. Computational method

The electronic energies and structures of the stationary species of interest in the gas phase and in acetonitrile were calculated by full optimization without any geometrical constraints using the density functional theory method with Gaussian 03 software and Becke's three-parameter hybrid functional (B3LYP) [18] with a 6-31 + g(d) basis set [19]. The nature of all the species was verified by calculating the vibrational frequencies [20,21]. The Polarized Continuum Model (PCM) of solvation was used to calculate the solvation energy in acetonitrile, and the charge densities of the complexes were obtained using natural population analysis [22–24].

3. Results and discussion

The photovoltaic performances of the D149/TEMPO-based DSSCs with LiTFSI or *x*BIs are shown in Fig. 1. The short-circuit current density (J_{sc}), open-circuit voltage (V_{oc}), fill factor (FF) and photovoltaic conversion efficiency (η) are listed in Table 1. Under standard global AM 1.5 solar conditions with a mask, the reference cell without any additives showed a J_{sc} of 4.21 mA cm^{-2}, an V_{oc} of 0.211 V and a FF 26.2, which corresponded to an overall conversion efficiency of 0.23%.

The addition of 1.2 M LiTFSI in the electrolyte led to an increase in the J_{sc} values: the J_{sc} reached 8.12 mA cm^{-2} with an V_{oc} of 0.69 V, and the energy conversion efficiency increased to 2.22%. It is known that due to the adsorption of Li^+ from the electrolyte, the band edge shifts downwards when a sufficient net number of positive charges are built up on the surface of the TiO_2 particles. The downward band-edge shift increased the charge injection efficiency of the excited state of the dye by shifting the conduction band edge to more positive potentials, which caused electron injection from the excited sensitizer and thus, an increase in the charge collection yield [25]. Because J_{sc} is dependent on both the rate of recombination and the band-edge position of TiO_2, an easy transfer from the positively shifted band-edge position of TiO_2 and the retarded recombination due to the barrier layer of Li^+ provided a significant increase in J_{sc}.

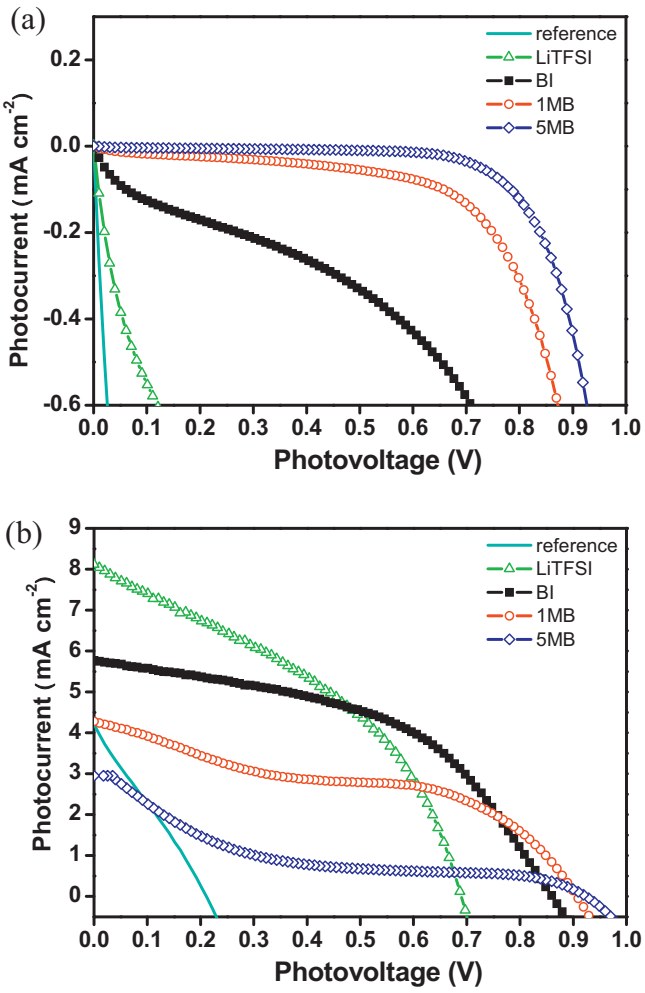

Fig. 1. Photocurrent density-potential characteristics of DSSCs with different additives (a) in the dark and (b) under simulated illumination (AM 1.5, 100 mW cm^{-2}) with masking.

The influence of benzimidazole additives on the DSSC performance was due to the electron donation ability of the nitrogen lone pairs in the benzimidazole ring, which can be estimated by the partial charge of the N atoms [26]. To estimate the extent to which the lone-pair electrons of the nitrogen atoms donate, the partial charges of the nitrogen atoms in position 3 of the *x*BI in acetonitrile were calculated from the optimized structure of *x*BI in acetonitrile by the theoretical approach. The charge of the N atom in position 3 of the *x*BI group is −0.565, −0.559 and −0.569 for BI, 1MB, and 5MB, respectively, suggesting that the *x*BI molecule adsorbs onto the free Lewis acid sites of the TiO_2 electrode [27]. It is known that the greater the partial charge of the N atom in the *x*BI group, the easier and more often the *x*BI can be adsorbed onto the Lewis acid sites of the TiO_2 surface [28].

The adsorption of *x*BI on the surface of the TiO_2 electrode provided a barrier layer for the surface of the TiO_2 particles, which could more efficiently suppress the dark current arising from the $TEMPO^+$ reduction by the conduction band electrons at the semiconductor-electrolyte junction, as shown in the *J*–*V* characteristics of the cells under dark conditions (Fig. 1b). Although the dark current is not an exact simulation of the recombination current under illumination due to the localized variation in the medium of the electrolyte and the potential distribution through the TiO_2 electrode, it can be used to estimate the extent of the reduction in the $TEMPO^+$ recombination with the conduction band electrons. The onset voltage of the cells increased in all cases with the addition of *x*BI, which showed that the addition of *x*BI reduced the electron recombination between the TiO_2 surface and $TEMPO^+$.

Table 2
Photovoltaic performance of DSSCs with different *x*BIs in LiTFSI/TEMPO/acetonitrile electrolytes.

0.5 M of	V_{oc} (V)	J_{sc} (mA cm^{-2})	FF	η (%)
None	0.690	8.12	39.6	2.22
BI	0.820	8.06	51.8	3.42
1MB	0.828	7.70	56.9	3.63
5MB	0.841	6.29	55.4	2.93

With the addition of *x*BI in the TEMPO/$TEMPO^+$ dissolved in acetonitrile, the V_{oc} increased from 0.211 V to 0.860, 0.907, and 0.924 V for BI, 1MB, and 5MB, respectively. The increased V_{oc} was due to the adsorption of basic *x*BI on the surface of TiO_2. A negative surface charge build-up can cause the band edges to shift upward toward negative electrochemical potentials. Because the value of V_{oc} is determined from the difference between the quasi-Fermi level of the TiO_2 film and the potential of the redox mediator in the electrolyte, under the assumption that the potential of the redox mediator remained constant with the addition, a negative shift in the conduction band edge of TiO_2 increased the V_{oc}.

From the measurement of the work function of the film, the Fermi-level shift (φ) at the FTO–TiO_2 interface was estimated to be φ = 5.93 V for the reference, and it changed to 5.95, 5.89 and 5.84 V with the addition of BI, 1MB and 5MB, respectively. The observed Fermi level in the order of BI > 1MB > 5MB with the addition of *x*BI, which is consistent with the value of V_{oc} within the error range.

Compared to the common Ru-based DSSCs, the detachment of the organic dye was observed with time, which showed that there is a competitive adsorption between the *x*BI and the D149 dye on the surface of TiO_2 particles in this system. To see the competitive detachment of the D149 dye from the TiO_2 particles in the presence of *x*BI in the electrolyte, UV/Vis measurements were conducted on the D149-attached TiO_2 film before and after contact with the *x*BI/acetonitrile or *x*BI/LiTFSI/acetonitrile solution for 1 h in a closed container, and the results are shown in Fig. 2. The dye detachment percentage is calculated using the equation: $100 \times (A_{before} - A_{after})/A_{before}$, where A_{before} and A_{after} are the absorbance of D149 at λ = 535 nm of the TiO_2 film before and after the contact with the *x*BI/acetonitrile (or *x*BI/LiTFSI/acetonitrile) solution. After 1 h of contact with the *x*BI/acetonitrile solution, almost all the D149-attached TiO_2 films showed a decreased UV absorption of D149, and this decrease was significant for the addition of 5MB in the electrolyte. Up to 20% dye loss was observed in the TiO_2 films when the D149-attached TiO_2 film was exposed to the 5MB/acetonitrile solution.

The dye detachment behavior was also observed in the presence of Li^+ in the electrolyte, i.e., *x*BI/LiTFSI/acetonitrile solution; however, the degree of detachment was lower than that in the *x*BI solution, which could be due to the specific properties of Li^+ in TiO_2 particles. It is known that Li^+ can be adsorbed on the surface of TiO_2, but it can also intercalate irreversibly into the TiO_2 lattice [29].

Following this result, the electrolyte composition for the reference was fixed to 0.5 M TEMPO, 0.025 M $NOBF_4$, and 1.2 M LiTFSI in acetonitrile, and 0.5 M of different *x*BI was added to observe the effect of the additives on the performance of DSSCs. The *J*–*V* curve is shown in Fig. 3. The values of J_{sc}, V_{oc}, FF and η with an additive in the electrolyte are listed in Table 2.

The inset in the figure shows the *J*–*V* characteristics of the cells under dark conditions. The onset voltage of the cells increased in the order of 5MB > 1MB > BI in the electrolytes, which suggested that the reduction in the electron recombination between the TiO_2 surface and $TEMPO^+$ is greater with the addition of 5MB than with the addition of BI. This result is consistent with the detachment

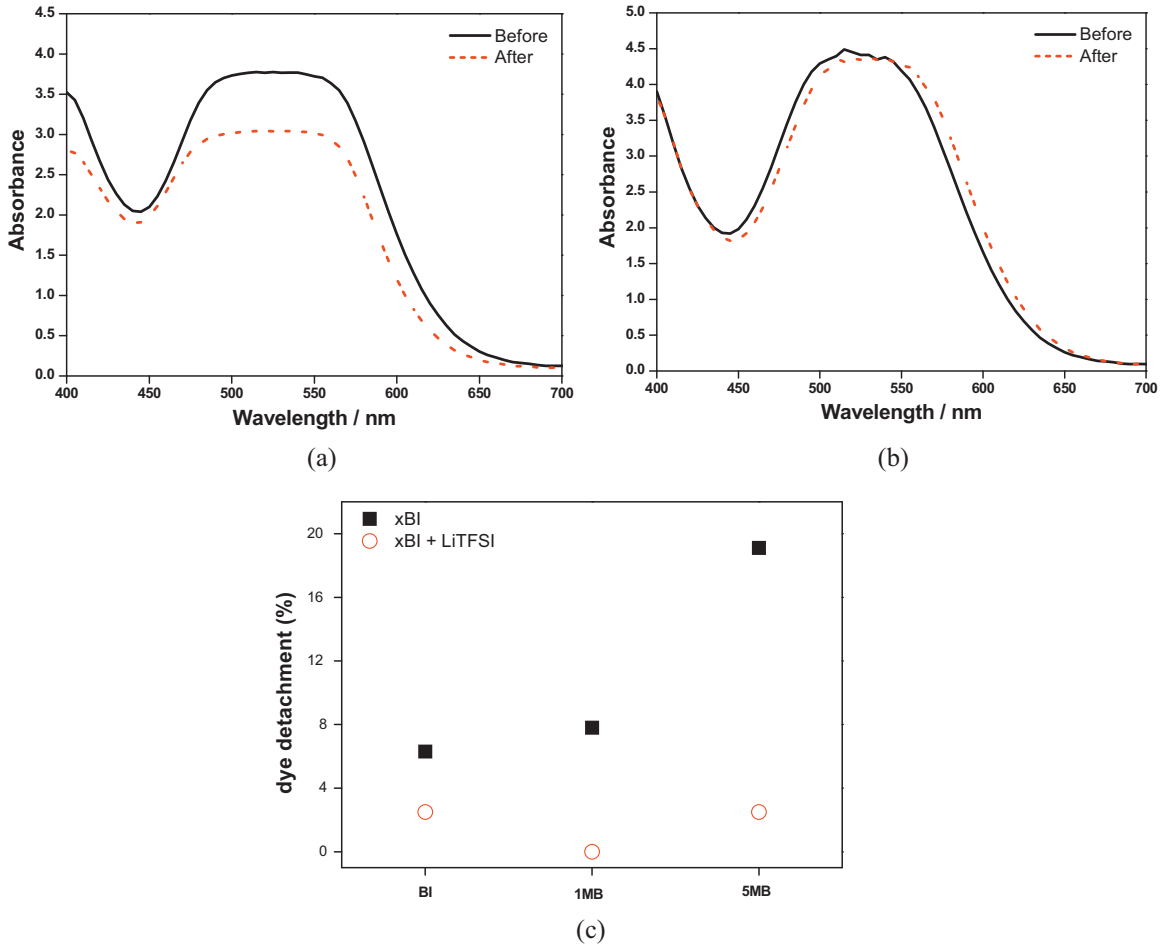

Fig. 2. UV absorption of the D149-TiO_2 electrode before and after contact with 0.5 M of (a) 5MB/acetonitrile and (b) 5MB/1.2 M LiTFSI/acetonitrile solution. (c) Detachment percentage of the D149-TiO_2 electrode before and after contact with the *x*BI/acetonitrile or *x*BI/LiTFSI/acetonitrile solution.

observation due to the *x*BI, i.e., the presence of 5MB in the electrolyte enhanced the detachment of the dye and formed a barrier layer on the surface of the TiO_2 particles with 5MB, which inhibited the electron recombination.

The addition of *x*BI reduced the electron recombination between the TiO_2 surface and $TEMPO^+$; therefore, the DSSC performance was enhanced, as demonstrated in Fig. 3. The negative shift of the band edges and the loss of sensitizers due to the competitive detachment at the surface of the TiO_2 particles in the presence of *x*BI in the electrolyte can explain the decreased J_{sc} value when *x*BI was added to the electrolyte. The presence of *x*BI in the TEMPO/$TEMPO^+$ electrolyte solution influenced the DSSC performance, especially the increase in the V_{oc} and η values of the solar cell compared to those of the DSSCs containing only Li^+ in the electrolyte. Among the additives tested in this study, either 1MB or BI resulted in the highest η, and this trend is consistent with the benzimidazole additive effect on the I^-/I_3^- redox couple in acetonitrile using the N719 dye [28].

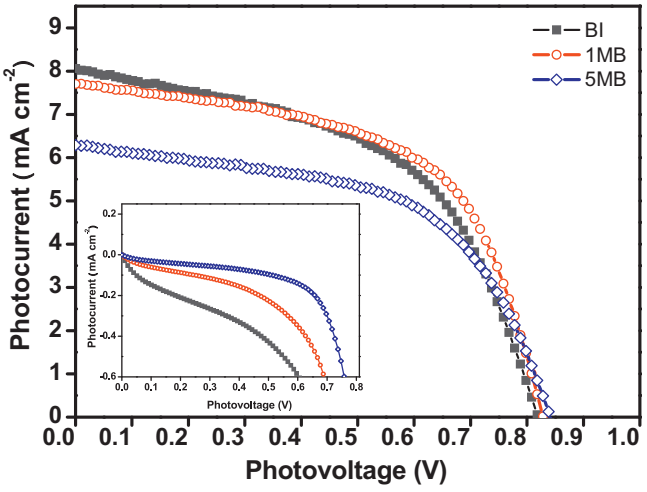

Fig. 3. Photocurrent density-potential characteristics of DSSCs with different *x*BIs in TEMPO/$TEMPO^+$/acetonitrile DSSCs.

The V_{oc} values for all the samples were lower than that without Li^+, which could be due to the strong adsorption of Li^+ on the surface of TiO_2. Because the adsorption of Li^+ is stronger than that of *x*BI, the addition of a co-adsorbent molecule (i.e., *x*BI) in the electrolyte could affect significantly the behavior of redox mediators (i.e., TEMPO/$TEMPO^+$) instead of that of TiO_2. Therefore, we studied the additive effect of the redox potential of TEMPO by CV measurements and a theoretical approach.

Because the concentration of *x*BI was same as that of TEMPO in the electrolyte, we assumed that all the *x*BIs affected the potential of TEMPO (or $TEMPO^+$). Therefore, the redox potentials of the TEMPO complexes with different *x*BIs can be calculated [30–32].

The nitroxide radicals (R_2N–$O^\bullet$) of the TEMPO redox mediator used in this research can be reversibly oxidized to the corresponding oxammonium cation (R_2N^+=O). For the nitroxides, the standard oxidation potentials were calculated relative to the SHE by deter-

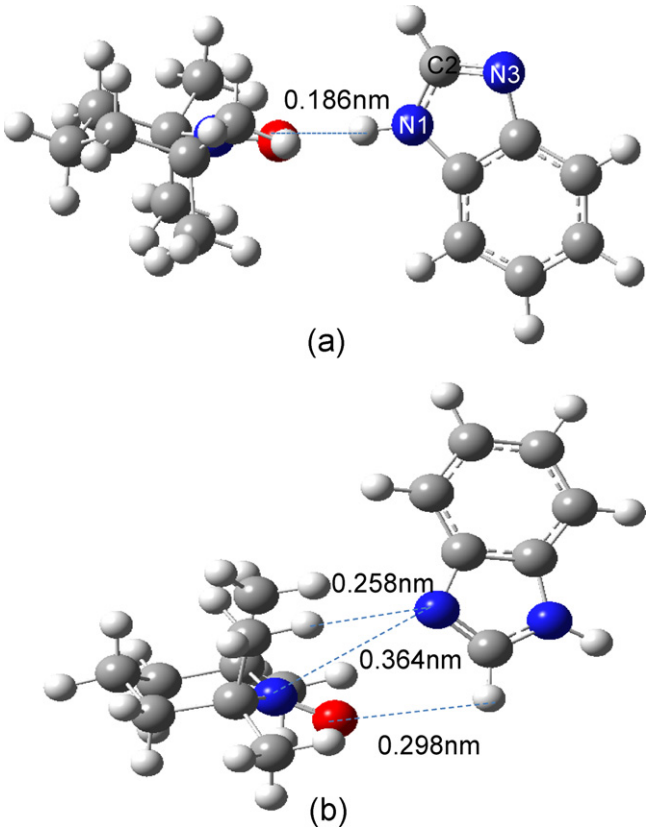

Fig. 4. Optimized B3LYP structures of (a) BI···TEMPO and (b) BI···TEMPO$^+$ complexes in acetonitrile calculated by the B3LYP/6-31 + g(d) basis set.

mining the Gibbs free energy of the following reaction:

$$R_2N\text{–}O^{\bullet}(sol) + H^+(sol) \rightarrow R_2N^+{=}O(sol) + 1/2H_2(gas) \quad (1)$$

The Gibbs energy change of the reaction can be written in two half reactions:

$$R_2N\text{–}O^{\bullet}(sol) \rightarrow R_2N^+{=}O(sol) + e^-(gas) \quad (2)$$

$$H^+(sol) + e^-(gas) \rightarrow 1/2H_2(gas) \quad (3)$$

The standard Gibbs energy is the sum of the Gibbs energy from Reactions (2) and (3).

$$\Delta G_1^\circ = \Delta G_2^\circ + \Delta G_3^\circ$$

The Gibbs free energy of Reaction (3), ΔG_3°, is reported as −4.36 V [32,33], and the value of ΔG_2° can be obtained from the calculated Gibbs energy of each component in the reaction.

The geometry of the neutral radicals and the positively charged oxidized species were optimized using the B3LYP/6-31 + g(d) method in acetonitrile. In each of the configurations, the N–O of the TEMPO was placed linearly with the C2–H of the BI or between the C2–H and N1–H of the BI: one horizontal and one vertical for the plane made by the benzimidazole ring. All four initial configurations were constructed for geometry optimization. The optimized B3LYP structures of BI···TEMPO and BI···TEMPO$^+$ complexes with most stable energy are shown in Fig. 4, and they indicate that there are nonbonding interactions between the BI and TEMPO (or TEMPO$^+$). The B3LYP structure of *x*BI···TEMPO (or TEMPO$^+$) was obtained with a similar approach, and an optimized structure was obtained with similar positions of the different *x*BIs on each TEMPO (or TEMPO$^+$). The solvent effect was calculated by the optimized gas phase geometry.

The oxidation potential can then be obtained using the following equation, where n is the number of electrons transferred (in this case $n = 1$), and F is the Faraday constant (96485.3383 C/mol):

$$\Delta G_1^\circ = nFE^\circ$$

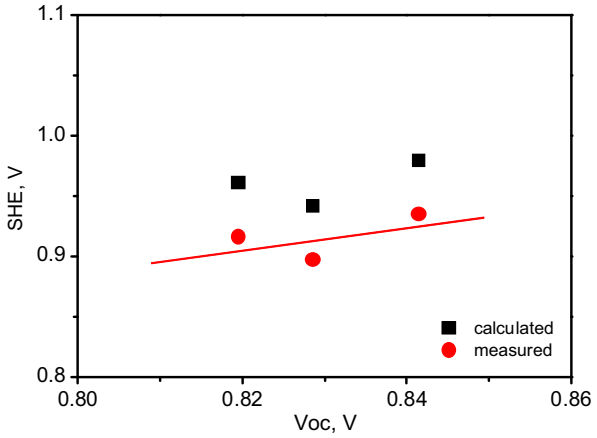

Fig. 5. Dependence of the V_{oc} of DSSCs and the SHE of the redox mediator in the presence of *x*BI, as determined by experimental and theoretical methods.

The calculated mediator potential, the measured value in the presence of *x*BI and the dependence of the V_{oc} are shown in Fig. 5. There is good agreement between the calculated and experimental potentials despite the relatively low basis set used in this theoretical approach to save the time and cost.

Under the assumption that the surface of the TiO_2 particle was covered by Li^+ and the band edge of the TiO_2 film was constant, the V_{oc} values depend on the electrochemical potential of the TEMPO/TEMPO$^+$ in the presence of the *x*BI. A similar trend between the SHE and the V_{oc} of DSSCs in Fig. 5 shows that the addition of *x*BI in the presence of Li^+ in the electrolyte improves the V_{oc} by changing the potential of the redox mediators.

In general, basic additives such as *x*BIs were added in the electrolytes without any serious consideration, and we found that the choice of adsorbent is significant for the long-term stability of organic dye-based solar cells. Therefore, more fundamental analysis is required when choosing the additives in electrolytes. In addition, theoretical calculations of the redox potentials of the redox mediators in the electrolyte indicated their importance in the design of additives with desirable redox properties, particularly for compounds in which complex chemical equilibria are known to hamper experimental measurements.

4. Summary

DSSCs were fabricated with an organic dye and a non-iodine redox mediator, and the effect of the *x*BI additives was investigated using the photovoltaic performance and theoretical calculations. The basicity of the *x*BI affected the adsorption onto the TiO_2 semiconductor particles in the DSSCs, which led to the detachment of the D149 organic dye from the TiO_2 particles. The addition of *x*BI in the presence of Li^+ in the electrolyte affected the potential of the TEMPO/TEMPO$^+$ redox mediators and improved the V_{oc} of the DSSCs compared to that of DSSCs with only Li^+ in the electrolyte, which was confirmed by CV measurements and theoretical calculations.

Acknowledgements

This work was supported by the Basic Science Research Program (no. 2010-0020918) and the Centre for Next-Generation Dye-sensitized Solar Cells (no. 2010-0001842) through the National Research Foundation of Korea (NRF) grant funded by

the Ministry of Education, Science and Technology (MEST) of Korea.

References

[1] A.B.F. Martinson, T.W. Hamann, M.J. Pellin, J.T. Hupp, Chem. Eur. J 14 (2008) 4458.
[2] A. Kay, R. Humphry-Baker, M. Graetzel, J. Phys. Chem. 98 (1994) 952.
[3] S. Ardo, G.J. Meyer, J. Chem. Soc. Rev. 38 (2009) 115.
[4] M. Wang, N. Chamberland, L. Breau, J.E. Moser1, R. Humphry-Baker, B. Marsan, S.M. Zakeeruddin, M Grätzel, Nat. Chem. 2 (2010) 385.
[5] G. Oskam, B.V. Bergeron, G.J. Meyer, P.C. Searson, J. Phys. Chem. B 105 (2001) 6867.
[6] P. Wang, S.M. Zakeeruddin, J.E. Moser, R. Humphry-Baker, M. Grätzel, J. Am. Chem. Soc. 126 (2004) 7164.
[7] H. Nusbaumer, J.E. Monser, S.M. Zakeeruddin, M.K. Nazeeruddin, M. Grätzel, J. Phys. Chem. B 105 (2001) 10461.
[8] S.A. Sapp, C.M. Elliott, C. Contado, S. Caramori, C.A. Bignozzi, J. Am. Chem. Soc. 124 (2002) 11215.
[9] S. Hattori, Y. Wada, S. Yanagida, S. Fukuzumi, J. Am. Chem. Soc. 127 (2005) 9648.
[10] Z. Zhang, P. Chen, T.N. Murakami, S.M. Zakeeruddin, M. Grätzel, Adv. Funct. Mater. 18 (2008) 341.
[11] T.S. Kang, K.H. Chun, J.S. Hong, S.H. Moon, K.J. Kim, J. Electrochem. Soc. 147 (2000) 3049.
[12] S.Y. Huang, G. Schlichthörl, A.J. Nozik, M. Grätzel, A.J. Frank, J. Phys. Chem. B 101 (1997) 2576.
[13] G. Schlichthörl, S.Y. Huang, J. Sprague, A.J. Frank, J. Phys. Chem. B 101 (1997) 8141.
[14] G. Boschloo, H. Lindström, E. Magnusson, A. Holmberg, A. Hagfeldt, J. Photochem. Photobiol. A: Chem. 148 (2002) 11.
[15] G. Boschloo, A. Hagfeldt, Chem. Phys. Lett. 370 (2003) 381.
[16] T.C. Tien, F.M. Pan, L.P. Wang, C.H. Lee, Y.L. Tung, S.Y. Tsai, C. Lin, F.Y. Tsai, S.J. Chen, Nanotechnology 20 (2009) 305201.
[17] H. Ishii, K. Sugiyama, E. Ito, K. Seki, Adv. Mater. 8 (1999) 605.
[18] A.D. Becke, J. Chem. Phys. 98 (1993) 5648.
[19] W.J. Hehre, L. Radom, P.V.R. Schleyer, J.A. Pople, Ab Initio Molecular Orbital Theory, J. Wiley. Sons, New York, 1986, 548.
[20] J.A. Pople, R. Krishnan, H.B. Schlegel, J.S. Binkley, Intern. J. Quantum Chem. 13 (1979) 225.
[21] J.A. Pople, H.B. Schlegel, R. Krishnan, D.J. Defrees, J.S. Binkley, M.J. Frisch, R.A. Whiteside, R.F. Hout, W.J. Hehre, Intern. J. Quantum Chem. 15 (1981) 269.
[22] S. Miertus, E. Scrocco, J. Tomasi, Chem. Phys. 55 (1981) 117.
[23] V. Barone, M. Cossi, J. Phys. Chem. A 102 (1998) 1995.
[24] M. Cossi, V. Barone, J. Phys. Chem. A 104 (2000) 10614.
[25] B. Shin, J. Won, T. Son, Y.S. Kang, C.K. Kim, Chem. Commun. 47 (2011) 1734.
[26] H. Kusama, H. Arakawa, J. Photochem. Photobiol. A: Chem. 160 (2003) 171.
[27] K. Nohara, H. Hidaka, Ezio. Pelizzetti, N. Serpone, J. Photochem. Photobiol. A: Chem. 102 (1997) 265.
[28] H. Kusama, H. Arakawa, J. Photochem. Photobiol. A: Chem. 162 (2004) 441.
[29] N. Kopidakis, K.D. Benkstein, J.v.d. Lagemaat, A.J. Frank, J. Phys. Chem. B 107 (2003) 8141.
[30] J.P. Blinco, J.L. Hodgson, B.J. Morrow, J.R. Walker, G.D. Will, M.L. Coote, S.E. Bottle, J. Org. Chem. 73 (2008) 6763.
[31] M. Namazian, H.A. Almodarresieh, M.R. Noorbala, H.R. Zare, Chem. Phys. Lett. 396 (2004) 424.
[32] J.L. Hodgson, M. Namazian, S.E. Bottle, M.L. Coote, J. Phys. Chem. A 111 (2007) 13595.
[33] P. Winget, C.J. Cramer, D.G. Truhlar, Theor. Chem. Acc. 112 (2004) 217.